

# Unique Twisted Ribbons Generated by Self-Assembly of Oligo(*p*-phenylene ethylene) Bearing Dimeric Bile Acid Pendant Groups

Yan Li,<sup>[a, b]</sup> Guangtao Li,<sup>\*[a]</sup> Xinyan Wang,<sup>[a, c]</sup> Weina Li,<sup>[a, b]</sup> Zhixiang Su,<sup>[a]</sup> Yihe Zhang,<sup>[a, c]</sup> and Yong Ju<sup>\*[a, b]</sup>

**Abstract:** A series of novel oligo(*p*-phenylene ethynylene) (OPE) derivatives bearing dimeric cholic acid (OPE1), deoxycholic acid (OPE2) and lithocholic acid (OPE3) was synthesized. The self-assembly behavior of these derivatives were systematically studied and compared in a THF/water solvent mixture. The addition of water to THF can induce the helical stacking

of oligo(*p*-phenylene ethylene) bearing dimeric deoxycholic acid end groups, which leads to highly interesting twisted assemblies. Variation of the bile acid group led to nanostructures with

**Keywords:** bile acids · chirality · conjugation · self-assembly · supramolecular chemistry

drastically different morphologies. The application of spectroscopy in combination with X-ray diffraction techniques provided a reasonable view of the final self-assembled structures. The observed distinctive aggregate shapes and the preference in the type of molecular packing of these steroid–OPE conjugates are attributed to the subtle differences in their molecular features.

## Introduction

The controlled organization of  $\pi$ -conjugated molecules into highly ordered arrays at the supramolecular level is of great importance, owing to the potential applications of these arrays in optical devices and supramolecular electronics.<sup>[1]</sup> Nature elegantly utilizes the self-assembly of biomolecules to construct functional superstructures. In a manner that mimics natural processes, the introduction of biogenetic

compounds (e.g., amino acids and nucleic acids) to  $\pi$ -conjugated systems provides one convenient way to create a variety of fascinating morphologies for the development of advanced materials.<sup>[2]</sup>

Steroids make up a class of naturally occurring compounds containing four fused rings, generally aliphatic rings, examples of which include the biologically important bile acids and cholesterol.<sup>[3]</sup> In addition to their physiological role, steroidal compounds have been presented as an inexpensive source of chirality. Due to the rigid steroidal skeleton and its hydrophobic nature, such molecules tend to form supramolecular aggregates in which the position and orientation of the molecule is well organized.<sup>[4]</sup> In this respect, cholesterol is widely used as a pendant group, which can be attached to  $\pi$ -conjugated systems to induce the chiral packing of chromophores.<sup>[5]</sup> However,  $\pi$ -conjugated compounds bearing dimeric bile acid moieties have been far less systematically investigated. In contrast to cholesterol, bile acids are strikingly diverse in nature; therefore, it is highly interesting to study and compare the self-assembly behavior of these structurally closely related compounds.

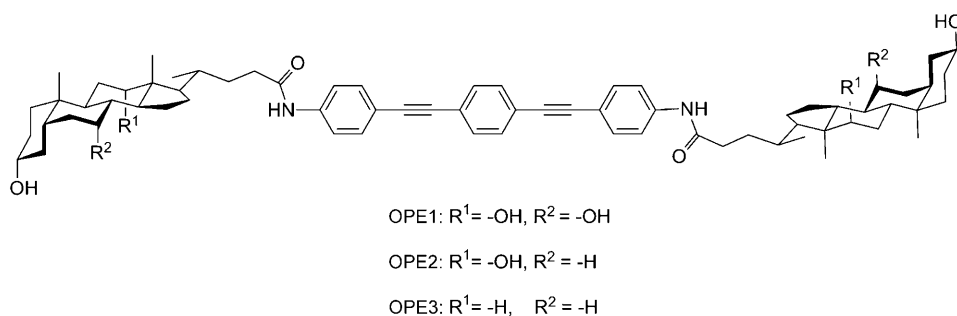
Herein, a new series of compounds consisting of an oligo(*p*-phenylene ethylene) (OPE) spacer and a bile acid end group was designed. Scheme 1 shows the synthesized OPE derivatives bearing dimeric cholic acid (OPE1), deoxycholic acid (OPE2), and lithocholic acid units (OPE3), which are differentiated only by the number of hydroxyl groups. Very interestingly, it was found that such subtle var-

[a] Y. Li, Prof. Dr. G. Li, X. Wang, W. Li, Z. Su, Prof. Dr. Y. Zhang, Prof. Dr. Y. Ju  
Department of Chemistry  
Key Lab of Organic Optoelectronics & Molecular Engineering  
Ministry of Education, Tsinghua University  
Beijing, 100084 (China)  
Fax: (+86)10-6279-2905  
E-mail: lgt@mail.tsinghua.edu.cn

[b] Y. Li, W. Li, Prof. Dr. Y. Ju  
Department of Chemistry  
Key Lab of Bioorganic Phosphorus Chemistry & Chemical Biology  
Ministry of Education, Tsinghua University  
Beijing, 100084 (China)  
Fax: (+86)10-6278-1695  
E-mail: juyong@mail.tsinghua.edu.cn

[c] X. Wang, Prof. Dr. Y. Zhang  
School of Material Science and Technology  
China University of Geosciences  
Beijing 100083 (China)

Supporting information for this article is available on the WWW under <http://dx.doi.org/10.1002/chem.200900484>.



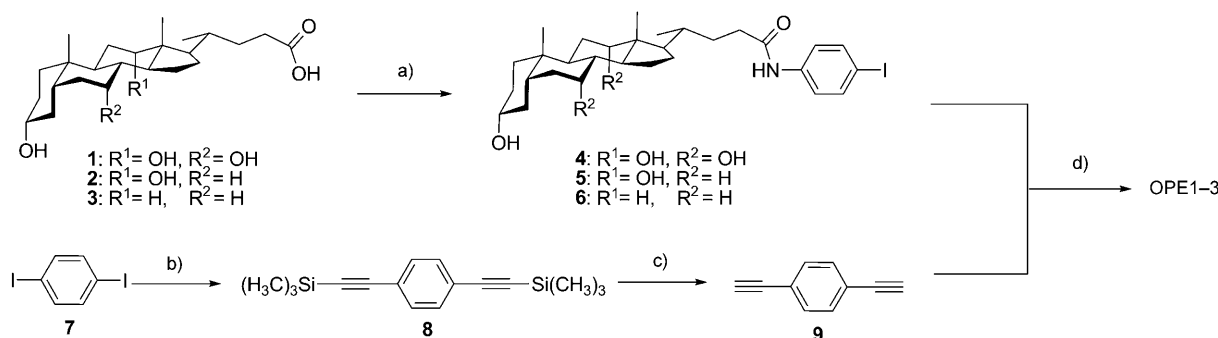
Scheme 1. Chemical structures of the synthesized OPEs bearing dimeric bile acid end groups.

iations could lead to nanostructures with drastically different morphologies.

## Results and Discussion

**Synthesis:** OPE derivatives OPE1, OPE2, or OPE3 were synthesized by Pd-catalyzed cross-coupling between the corresponding steroidal iodobenzene derivatives and 1,4-diethylbenzene (Scheme 2). The synthetic process was quite straightforward, and the structures of these compounds were confirmed by IR and NMR spectroscopies and mass spectrometry.

**Optical and self-assembly properties:** Because many dimeric cholesterol-based  $\pi$ -conjugated compounds are recognized as powerful gelling agents,<sup>[5]</sup> we first focused our attention on using these OPE derivatives as potential gelators. Various nonpolar solvents (such as cyclohexane, benzene, and alkyl halides) as well as several polar solvents (such as ethanol and THF) were tested, but to our disappointment, none of the bile acid derived OPEs formed a stable gel in these solvents. In fact, these compounds were either insoluble or precipitated upon cooling in most nonpolar (e.g., alkyl halides and aromatic solvents) and protic solvents (e.g., ethanol and water). However, except for OPE3, the new OPEs have rather high solubility ( $>6 \text{ mg mL}^{-1}$ ) in several aprotic polar solvents, such as THF and DMF, and form a clear light-yellow solution in these solvents with blue fluorescence.



Scheme 2. The synthetic route to OPEs bearing dimeric bile acid pendant groups. a) dicyclohexylcarbodiimide (DCC), 1-hydroxybenzotriazole (HOBT), 4-iodoaniline, RT; b) tetramethylsilane (TMS), [Pd(PPh<sub>3</sub>)<sub>4</sub>], CuI, Et<sub>3</sub>N, DMF, 60 °C; c) CH<sub>3</sub>OH, K<sub>2</sub>CO<sub>3</sub>, RT; d) [Pd(PPh<sub>3</sub>)<sub>4</sub>], CuI, (iPr)<sub>2</sub>NH, THF.

Hence, OPE1–OPE3 are either too soluble or too crystalline for gel formation.<sup>[6]</sup>

These results and the facially amphiphilic character of bile acids prompted us to investigate the self-assembly of OPE1–OPE3 in a mixed solvent. Recently, we found that gradually adding water to THF (which reinforces the hydrophobic interactions without blocking the formation of hydrogen bonds) is an ideal methodology

to induce the self-assembly of conjugated polymers bearing bile acid pendant groups.<sup>[7]</sup> One or two water molecules might also be present and may act as bridging groups between cholate hydroxyl groups, as is observed in the crystal structure of cholic acid.<sup>[8]</sup> This work inspired us to adopt a THF/water solvent system to study the self-assembly of OPE1–OPE3.

As water was gradually added, transparent solutions of OPE1 and OPE2 in THF both change into cloudy liquids that exhibit light scattering, which is indicative of the formation of nano- or micrometer aggregates. However, the resulting solution of OPE2 was much more turbid than that of OPE1 (Figure S1 in the Supporting Information). The concentration of both compounds in THF was identical ( $2 \times 10^{-4} \text{ M}$ ), thus this decrease of transparency is likely to result from the formation of larger aggregates. Indeed, dynamic light scattering (DLS) experiments revealed that OPE1 forms particles of the size in the range of 155–309 nm, with peak intensity at 230 nm and a polydispersity of 0.13. In contrast, the supramolecular aggregation of OPE2 is larger than 2  $\mu\text{m}$ , which is out of the range for our DLS measurement (Figure S2 in the Supporting Information).

Optical spectroscopies (UV/Vis, circular dichroism, and fluorescence spectroscopies) were used to study the formation of the aggregates and excimers in the solvent/nonsolvent mixtures used. Figure 1a and b show that the solvent-dependent UV/Vis spectra of OPE1 and OPE2 do not differ significantly. In absolute THF at 20 °C, absorption maxima for both compounds were at about 343 nm. Upon addition

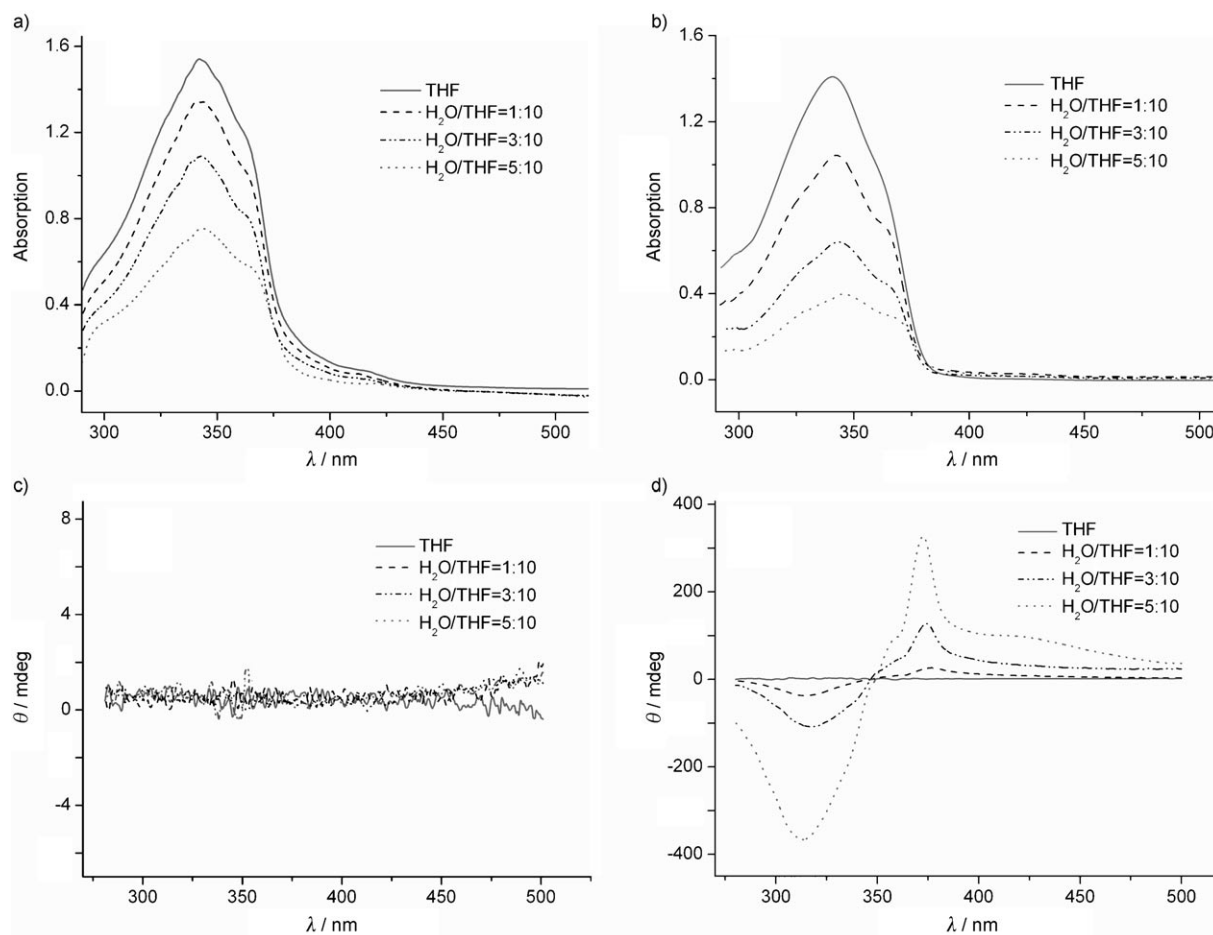


Figure 1. Absorption spectra of a) OPE1 and b) OPE2 in THF with increasing amounts of water; CD spectra in THF with increasing amounts of water of c) OPE1 and d) OPE2.

of water, at a rate of 10% per minute under vigorous stirring, the absorption intensity decreased considerably. Meanwhile, the appearance of a vibrational fine shoulder structure at  $\lambda = 366$  nm became much more clear in the aggregation state, which indicates the increase of effective conjugation length and the conformational order in the assemblies. Similar phenomena were also observed for other  $\pi$ -conjugated systems such as polythiophene and oligo(*p*-phenylene vinylene) in a THF/water system, indicating that changing the solvent polarity can affect the delicate conformation of the chromophores.<sup>[9]</sup> Although both of these compounds show decreases in absorption intensity, the decrease in OPE1 was relatively less significant than that of OPE2. Furthermore, an 8 nm redshift of the maximum was observed in the case of OPE2, which indicates that a J-type packing of OPE moieties exists in the formed assemblies. However, the wavelength shift of OPE1 was negligible, suggesting that the packing of the chromophores in OPE1 was less tight than OPE2. A striking consequence of the different arrangements of chromophores in these two compounds is the disparity in the circular dichroism (CD) spectra (Figure 1c and d). The CD silence of OPE1 reveals that it is not able to form helical aggregates in THF/water solution. On the con-

trary, the CD signal of OPE2 shows a positive Cotton effect in THF/water solution with the  $\theta = 0$  crossing wavelength near the absorption maximum (340 nm). With the incremental addition of water, the CD signal becomes remarkably stronger, indicating that the chromophores of OPE2 self-assembled in a helical sense. The CD spectra in THF with an increasing percentage of methanol were also measured. Although OPE2 is not soluble in methanol, no apparent Cotton effect was observed. The hydrophobic interaction in methanol is less significant than that in water, which may hinder the extended packing of molecules for the formation of chiral aggregates.

The remarkable different experimental phenomena and optical observations were also reflected by the distinctive morphologies of OPE1 and OPE2 observed by using SEM and TEM. As demonstrated in Figure 2a, in THF/water solution, OPE1 afforded spherical particles with diameters ranging from 120 to 250 nm. The particles form opening holes on their surfaces, which indicated that they had a hollow interior. The majority of these vesicles tended to stick together and were approximately 10–30 nm larger in diameter than the typical micelle size derived from common surfactants.<sup>[10]</sup> Moreover, many other vesicles self-assembled

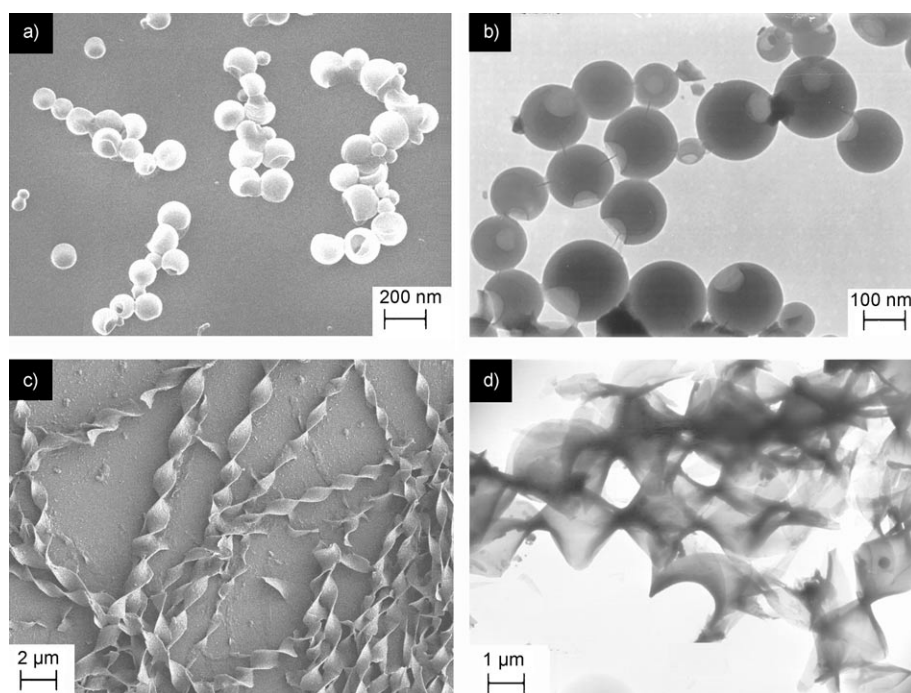


Figure 2. SEM and TEM images of supramolecular assemblies of OPE1 (a, b) and OPE2 (c, d) in water/THF (1:2 v/v).

from small amphiphilic molecules immediately collapsed on solid surfaces,<sup>[11]</sup> but these OPE vesicles showed remarkable stability and retained their shape upon drying, presumably due to the rigid  $\pi$ -conjugated spacer and the steroid nuclei. The TEM image in Figure 2b further confirmed these robust capsule-like aggregates with diameters of about 200 nm, which is in agreement with the DLS experimental results.<sup>[12]</sup> It is interesting to note that this linear structure leads to a spherical morphology.

On the other hand, OPE2, with dimeric deoxycholate moieties, shows a very interesting assembly behavior in water/THF (1:2 v/v): remarkably broad ribbons twisted in a right-handed helical structure were observed (Figure 2c and d). The ribbons are approximately 1.5  $\mu\text{m}$  wide and a few hundred micrometers in length, with an average helical pitch length of 2  $\mu\text{m}$ . Moreover, the dimensions of these supramolecular aggregations were large enough to be observed by using normal optical microscopy (Figure 3), which provides a convenient approach to capture the image of these twisted ribbons in situ. Polarizing microscopy shows that periodic color strips appear on the self-assembled twisted ribbons, which suggests the existence of a periodic ordered packing of molecular structures. The twisted ribbons derived from OPE2 exhibited strong blue fluorescence that can be clearly detected by fluorescent optical microscopy (Figure 4a). The fluorescent spectra of the aggregate state were slightly broader and exhibited a redshift ( $\sim 6$  nm) compared with those observed in THF, which is indicative of a J-type packing of  $\pi$ -conjugated chains in the molecular assemblies (Figure 4b).

We wondered how the presence of nonsolvent could affect the morphological transition of OPE2 that finally leads to such a unique microstructure. To address this question, the self-assembly of OPE2 in THF ( $2 \times 10^{-4}$  M) with increasing addition of water was monitored by SEM (Figure 5). At the 5% volume fraction of water, bundle-like structures with a diameter of less than 1  $\mu\text{m}$  were found to be the dominant morphology. These bundles have a low aspect ratio and possess several branches at their ends, which is in sharp contrast to the nanofibers formed by similar cholesterol derivatives.<sup>[5,13]</sup> Upon increasing the water content to 20%, the twisted sense seems to start to form from the tips of the branches. In the meantime, the diameter of the bundles was increased considerably and leads to a ribbon-like structure. Further increasing the volume of water to 30% finally yields helical ribbons with an almost regular pitch length of 2  $\mu\text{m}$ , in line with the strong positive cotton effect observed in the CD spectrum.

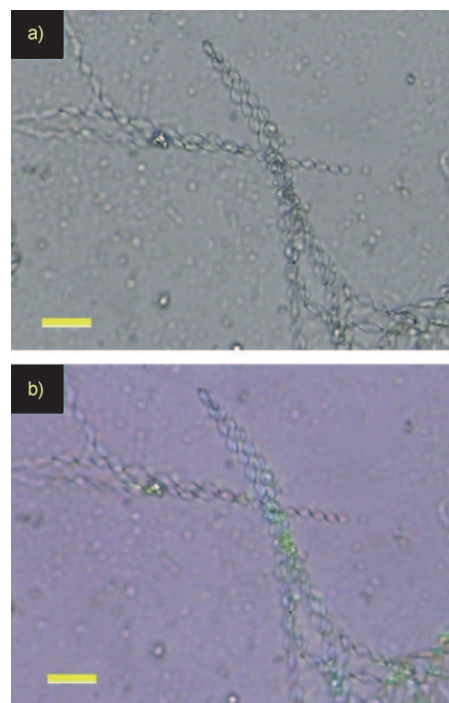


Figure 3. Photographs (1000 $\times$  magnification) of the twisted ribbons in water/THF 1:2 observed by optical microscopy under a) white light and b) polarized light. The scale bar is 10  $\mu\text{m}$ .

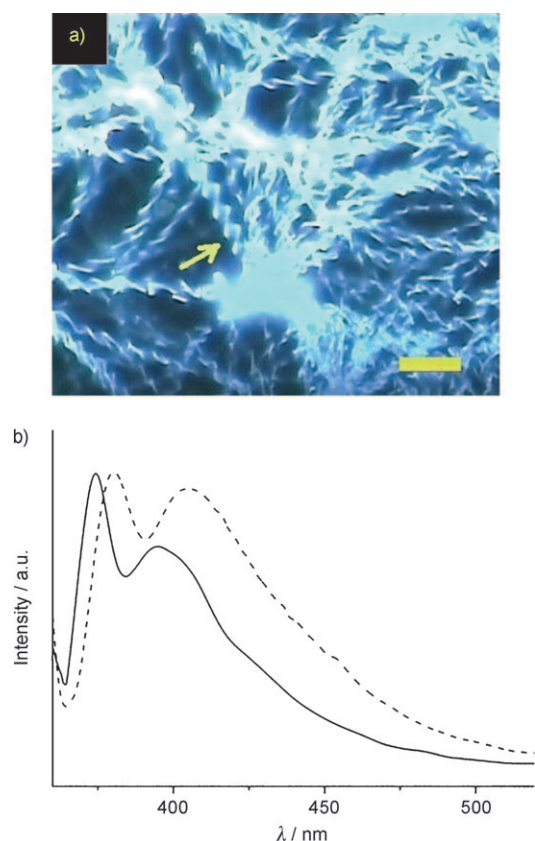


Figure 4. a) Photographs ( $1000\times$  magnification) of the twisted ribbons observed under illumination with 330–380 nm UV light. The arrow indicates the helical sense. The scale bar is  $10\ \mu\text{m}$ . b) Normalized emission spectra of OPE2 in THF solution (solid line) and in aggregation state (dashed line).

The progressive changes of the aggregate morphologies with the addition of water indicate that a relaxation process may be involved throughout the entire assembly.<sup>[14]</sup> In fact, the relaxation process is evidenced by the fact that when OPE2 was directly dissolved in a fixed ratio of THF/water mixture at elevated temperature, it did not yield any helical structure upon cooling (Figure S3 in the Supporting Information). In our experiment, it seems that the incremental addition of water to THF under ultrasound irradiation or vigorous stirring is necessary for the formation of these twisted ribbons. Even though bile acids possess more than ten chiral carbon atoms, the transfer of chirality from the molecular level to helical structures on a supramolecular scale that can be clearly visualized using techniques such as SEM, TEM, and even optical microscopy makes this system really unusual.

In contrast to OPE1 and OPE2, OPE3 (which possesses only two hydroxyl groups) yields large microcrystalline rods under the same conditions (Figure S4 in the Supporting Information). This compound is so insoluble in aqueous media that the addition of water leads to rapid precipitation.

**Mechanism of self-assembly:** The mechanism for the formation of the described superstructures is at present not very clear. The molecular structure of bile acid is considerably

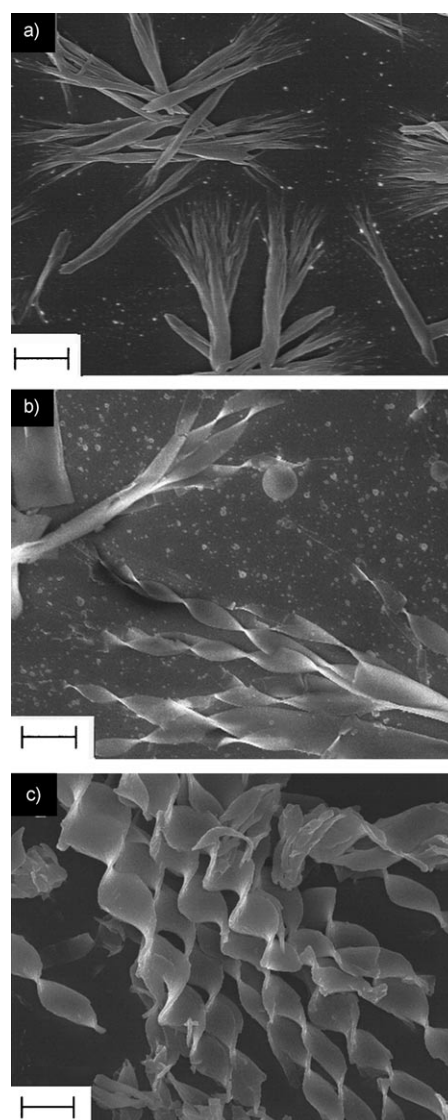
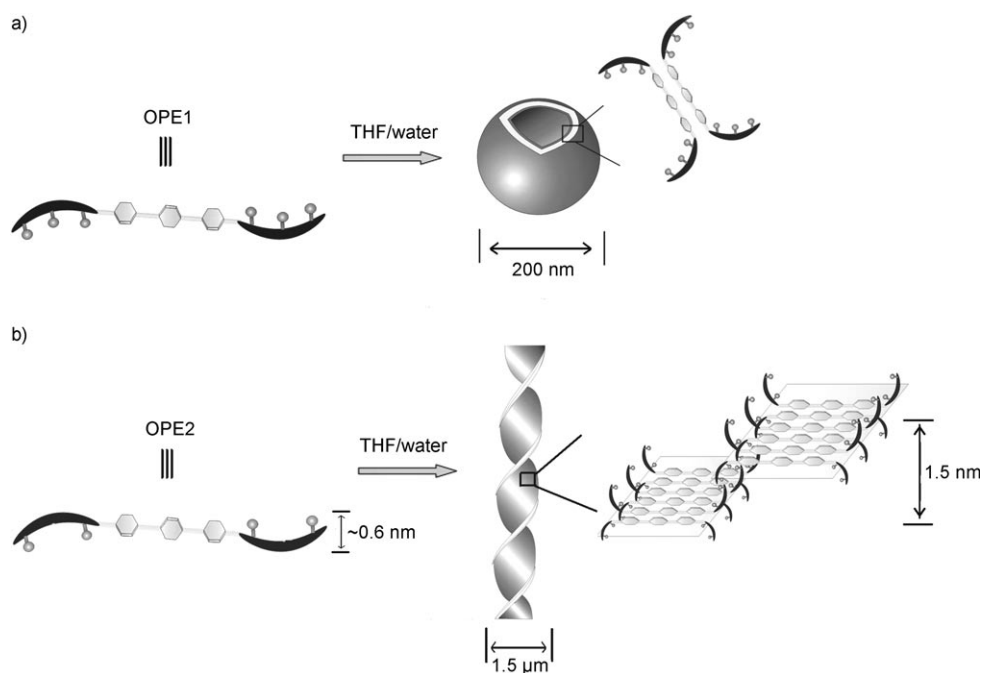


Figure 5. SEM images of hierarchical superstructures of OPE2 in THF/water solution with a volume fraction of water of a) 5%, b) 15%, and c) 30%. The scale bar is  $2\ \mu\text{m}$ .

different from conventional surfactants and the mechanism of their formation is quite complex, often involving complicated “secondary assemblies”.<sup>[15]</sup> As mentioned above, the spectroscopy studies (UV/Vis, CD, and fluorescence) demonstrate that OPE-derived steroidal compounds undergo extensive conformational changes in solvent/nonsolvent (THF/water) mixtures. It is believed that the cooperation of aromatic stacking, hydrogen bonding, and van der Waals interactions contributes significantly to the observed unique mesoscopic structures, whereas the orientation of the chromophore plays a crucial role in the optical and chiroptical properties. With reference to the existing literature, possible molecular packing models for the superstructures formed from OPE1 and OPE2 are suggested (Scheme 3).

As demonstrated in Scheme 3a, OPE1 possesses a  $\pi$ -conjugated spacer (OPE) and two amphiphilic pendant groups



Scheme 3. The proposed molecular packing models for a) OPE1 and b) OPE2.

(cholate). In the process of self-assembly, the hydrophobic OPE spacer should be arranged inside the membrane of the vesicles by  $\pi$ - $\pi$  stacking, whereas the relatively polar cholate groups should be exposed to the solvent. This is similar to the packing model of  $\pi$ -conjugated, macrocycle-derived vesicles reported by Tew et al.<sup>[16]</sup> It is reasonable that the hydro- and lipophilic sides of cholic acid meet together to yield a continuous membrane structure. If this is the case, there would be many hydroxyl groups on the surface of the membrane, which is consistent with the fact that the vesicles tend to stick together due to the formation of hydrogen bonds.

OPE2 displays several characteristics that are common with many other compounds that yield helical aggregates, such as chirality,  $\pi$  stacks, and the ability to form intermolecular hydrogen bonds, so we initially speculated that the superhelix mechanism may be quite general. However, after we carefully studied the molecular structure of deoxycholic acid, the self-assembly mechanism is probably a little different from its cholesterol analogue. Unlike cholesterol, bile acid possesses a curved backbone with the thickness of about 0.6 nm (C3-C18).<sup>[17]</sup> To make the extended packing of chromophores possible, the deoxycholate moieties could favor an interdigital conformation in which the adjacent molecules point in opposite directions. The exposed deoxycholate units may also interact with deoxycholates from other strings and form hierarchical secondary assemblies. Such packing leads to a helical arrangement of the molecules owing to the steric hindrance and the chirality of the steroid (Scheme 3b). The propensity of OPE2 to form large ribbon-like assemblies could also be enhanced by the planarization of OPE moieties, which confines the three benzene

groups to one aromatic platform, thereby maximizing the  $\pi$ - $\pi$  interaction. This conformation transition was clearly reflected on the UV/Vis spectrum by the enhanced absorption shoulder at approximately  $\lambda = 370$  nm.

The proposed mechanisms were supported by the wide-angle X-ray diffraction (WAXD) pattern of the supramolecular assemblies formed (Figure 6). X-ray diffraction of the vesicles formed from OPE1 shows peaks at 10.11, 18.94, and 22.56 in the range of  $2\theta = 3$ – $30^\circ\text{C}$ , which correspond to the distances of 8.78, 4.67, and 3.96 Å, respectively. Theoretically, the distance between the  $\pi$  stacking of OPEs is estimated to be about 0.4 nm<sup>[18]</sup> and the other  $d$  values were very close to the results obtained by Osada et al. in the investigation of giant needles formed by bile acid complex.<sup>[19]</sup> So the ob-

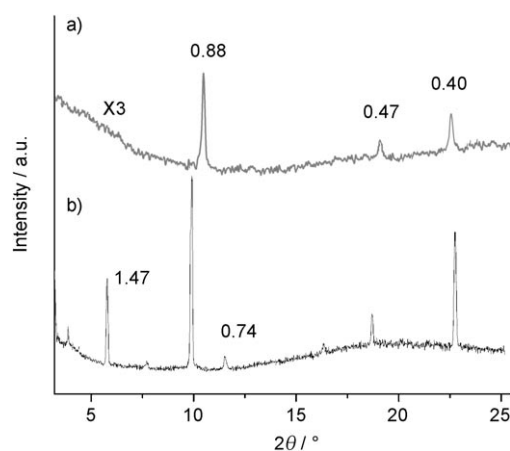


Figure 6. Proposed molecular packing models for a) OPE1 and b) OPE2.

served  $d$  spacings of 8.78 and 4.67 Å are possibly caused by the ordered packing of the adjacent cholate units, whereas the  $d$  spacing of 0.40 nm is a result of the center-to-center distance between the OPE spacers. In other words, this self-assembly aggregation preserved some of the basic packing patterns of bile acid, combined with the  $\pi$ - $\pi$  stacking of OPE moieties. The X-ray pattern of OPE2 was similar to that of OPE1, and several peaks appeared in the same range. It is interesting to note that the peaks corresponding to 1.47 and 0.74 nm (1.47/2) were not observed for OPE1. This periodicity indicates a lamellar packing structure. Considering that the space between the amide group (C24 atom) and the end of the steroid nucleus (C3 atom) is about 1.5 nm, based on the assumption that the alkyl spacer takes a fully extended conformation, the distance of 1.47 nm very likely corresponds to the distance between the planes formed by adjacent OPE strips, which gives clear evidence for the proposed self-assembly pattern of OPE2. The helical ribbons of OPE2 were solely right-handed, presumably reflecting the characteristic asymmetric nature of the deoxycholic acid. In our experiment, we also noticed that the signal-to-noise ratio of OPE1 in the XRD result was consistently lower than that of OPE2, which suggests that the molecules packing in the membrane of the vesicle were less organized than the twisted ribbons.

The distinctive self-assembly behavior of bile acid derived OPEs also raised the question of why the helical twist deteriorated when the number of hydroxyl groups either increased or decreased. To approach this question, it is essential to analyze the molecular arrangements in the supramolecular assemblies and the structures of these OPE derivatives. According to the molecular packing model proposed, one significant difference between these two supramolecular assemblies is that more steroid moieties in the vesicles are exposed to the solvent media than in the twisted ribbons in the every unit volume. In other words, many deoxycholic acid units were buried inside the large ribbon rather than in direct contact with the solvent. On the other hand, OPE1 has more hydroxyl groups on the cholate unit than OPE2, which makes the pendant groups of OPE1 more hydrophilic than their OPE2 counterparts. Considering the fact that the solvent used (THF/water mixture) is a relatively polar medium, it is reasonable that the pendant groups in OPE2 tend to be less exposed to the solvents than those in OPE1, which facilitates the reduction of the interfacial energy.

In the case of OPE3, the lack of hydrophilic functional groups means that the hydrophobic interactions of the large hydrophobic steroid nuclei become the dominant force, leading to either crystallization or precipitation. There is also a stronger tendency for growth in a one-dimensional fashion and loss of the curvature of the aggregates.

The number, location, and configuration of the hydroxyl groups play a crucial role in the formation of aggregates from bile acid derivatives.<sup>[20]</sup> In particular, two research groups found that among seven kinds of bile acid salts, only sodium deoxycholate aggregated in aqueous solution. In this case, an elongated right-handed helical structure with mac-

romolecular dimensions (10–100 Å) was obtained.<sup>[21]</sup> Compared with our result, we do not know whether the special behavior of deoxycholic acid is a coincidence. The backbone of deoxycholic acid presumably possesses an “appropriate” hydrophilic–hydrophobic balance, which may endow delicate influences on hydrogen-bond formation and hydrophobic interactions in aqueous solution. However, understanding and predicting the intermolecular forces in these complex systems and how it determines their self-assembly morphology remains a significant challenge.

## Conclusions

The current work employs naturally occurring bile acids as chirality-inducing moieties and offers a new means to control the packing and orientation of the chromophore. Very interesting is that subtle structure variations could drastically change the morphologies of the nanostructures formed. In this respect, it is possible to prepare many other interesting bile acid based molecular assemblies for this purpose by varying the type of bile acids and  $\pi$ -conjugated bridging groups of the scaffold. Based on the study of the self-assembly behavior of these structurally closely related compounds, this work provides new insights into the formation of chiral supramolecular assemblies starting from the molecular chirality of steroids. On the other hand, the microstructures formed from them may find use in hybrid-material synthesis or as a useful chiral medium for manipulating chemical separations. Some of these possibilities are being explored in our laboratory.

## Experimental Section

**Instruments:** <sup>1</sup>H NMR spectra were recorded at 300 MHz on JOEL JNM-ECA 300 spectrometers. Chemical shifts ( $\delta$ ) are given in ppm relative to TMS ( $\delta=0.0$ ). High-resolution electrospray ionization mass spectrometry (HRMS) measurements were recorded on a Bruker APEX spectrometer in positive mode. UV/Vis characterization was carried out on a Perkin–Elmer Lambda35 spectrometer. The fluorescence emission measurements were carried out using a Hitachi F-4500 fluorescence spectrometer. CD results were obtained on a Jasco-720 spectrometer. IR spectra were recorded on an AVATAR 360 ESP FTS spectrophotometer with KBr pellets. Elemental analyses were performed on a Carlo–Erba-1106 instrument. DLS measurements were carried out by using a Malvern Zetasizer 3000HS instrument, which supplies vertically polarized light with a wavelength of 633 nm. SEM experiments were performed with a LEO-1530 scanning electron microscope. TEM was performed on a MODEL H-800 electron microscope. All of the samples were stained with 1.5% phosphotungstic acid hydrate and filter paper was used to drain the excess solution. The polarizing behavior of the self-assembled aggregates and the fluorescence images were observed by using an Olympus 146 Tokyo incident-light optical microscope ( $\times 1000$  magnification).

**X-ray diffraction:** The vesicles and helical assemblies formed by OPE1 and OPE2 in solution were placed directly on the glass plate and dried in air. Both diffraction patterns were recorded on a Rigaku D/max diffractometer by using a  $\text{Cu}_{\text{K}\alpha}$  X-ray irradiation source (40 kV, 30 mA). Data were measured at room temperature between 3 and 30° in  $2\theta/\theta$  scan mode and the scanning rate was kept at 1° min<sup>-1</sup>.

**Chemicals:** Cholic acid, deoxycholic acid, lithocholic acid, and 4-iodoaniline were purchased from Sigma and used as received. Trimethylsilylacetyleylene was purchased from Shanghai Reagent Coporation.  $[\text{Pd}(\text{PPh}_3)_4]$  was obtained from Pingyang Chemical Company and washed with cold ethanol prior to use to remove the oxidized impurity. Other reagents and solvents were received from Beijing Chemical Company without further purification unless otherwise stated. 1,4-Diethynylbenzene was prepared and characterized according to a previously published procedure.<sup>[22]</sup>

**N-Cholyl-4-iodoaniline 4:** Cholic acid (818 mg, 2.0 mmol), HOBT (297 mg, 2.2 mmol), and 4-iodoaniline (438 mg, 2.0 mmol) were dissolved in  $\text{CH}_2\text{Cl}_2/\text{pyridine}$  (12 mL, 5:1 v/v). After stirring at 0°C for 10 min, DCC (453 mg, 2.2 mmol) was added and the resulting reaction mixture was kept at ambient temperatures for a further 20 h. A white precipitate was filtered from the purple solution and washed with acetone. The crude product was purified by column chromatography on neutral  $\text{Al}_2\text{O}_3$  (5%  $\text{MeOH}/\text{CH}_2\text{Cl}_2$ ) to obtain **4** (926 mg, 76%). <sup>1</sup>H NMR (300 MHz,  $[\text{D}_6]\text{DMSO}$ ):  $\delta$  = 9.58 (s, 1H; NH), 7.52 (d,  $J$  = 7.2 Hz, 2H; Ar-H), 7.42 (d,  $J$  = 7.2 Hz, 2H; Ar-H), 3.90 (s, 1H; 12-CH), 3.74 (s, 1H; 7-CH), 3.39–3.55 (m, 1H; 3-CH, overlap with the water signal in  $[\text{D}_6]\text{DMSO}$ ), 1.01–2.39 (m, 27H; alkyl-H), 1.01 (d,  $J$  = 6.0 Hz, 3H; 21- $\text{CH}_3$ ), 0.87 (s, 3H; 19- $\text{CH}_3$ ), 0.61 ppm (s, 3H; 18- $\text{CH}_3$ ); <sup>13</sup>C NMR (300 MHz,  $[\text{D}_6]\text{DMSO}$ ):  $\delta$  = 172.5, 139.0, 137.1, 121.4, 85.7, 72.1, 71.1, 67.3, 46.4, 46.1, 41.4, 35.2, 35.1, 34.7, 34.5, 33.7, 31.3, 30.3, 28.3, 27.3, 26.1, 24.6, 23.0, 22.4, 17.2, 12.4 ppm; HRMS (ESI):  $m/z$  calcd for  $[\text{C}_{30}\text{H}_{44}\text{INO}_4+\text{Na}]^+$ : 632.2213; found: 632.2200.

**N-Deoxycholyl-4-iodoaniline 5:** Compound **5** was synthesized as described for compound **4** by using deoxycholic acid instead of cholic acid. Yield: 77%; <sup>1</sup>H NMR (300 MHz,  $[\text{D}_6]\text{DMSO}$ ):  $\delta$  = 9.58 (s, 1H; NH), 7.52 (d,  $J$  = 7.2 Hz, 2H; Ar-H), 7.42 (d,  $J$  = 7.2 Hz, 2H; Ar-H), 3.90 (s, 1H; 12-CH), 3.74 (s, 1H; 7-CH), 3.39–3.55 (m, 1H; 3-CH, overlap with the water signal in  $[\text{D}_6]\text{DMSO}$ ), 1.01–2.39 (m, 27H; alkyl-H), 1.01 (d,  $J$  = 6.0 Hz, 3H; 21- $\text{CH}_3$ ), 0.87 (s, 3H; 19- $\text{CH}_3$ ), 0.61 ppm (s, 3H; 18- $\text{CH}_3$ ); <sup>13</sup>C NMR (300 MHz,  $[\text{D}_6]\text{DMSO}$ ):  $\delta$  = 172.4, 139.8, 137.4, 121.7, 86.7, 71.5, 70.5, 55.4, 48.0, 46.7, 46.5, 42.1, 36.8, 36.2, 35.7, 35.6, 34.3, 34.0, 33.5, 31.8, 30.8, 30.0, 27.7, 27.5, 26.7, 24.1, 23.6, 22.4, 17.6, 13.0 ppm; HRMS (ESI):  $m/z$  calcd for  $[\text{C}_{30}\text{H}_{44}\text{INO}_3+\text{H}]^+$ : 594.2444; found: 594.2439.

**N-Lithocholyl-4-iodoaniline 6:** Compound **6** was synthesized as described for compound **4** by using lithocholic acid instead of cholic acid. Yield: 80%; <sup>1</sup>H NMR (300 MHz,  $[\text{D}_6]\text{DMSO}$ ):  $\delta$  = 9.95 (s, 1H; NH), 7.60 (d,  $J$  = 7.2 Hz, 2H; Ar-H), 7.41 (d,  $J$  = 7.2 Hz, 2H; Ar-H), 4.44 (brs, 1H; OH), 3.39–3.55 (m, 1H; 3-CH, overlap with the signal of water in  $[\text{D}_6]\text{DMSO}$ ), 1.05–2.35 (m, 28H; alkyl-H), 1.01 (d,  $J$  = 6.0 Hz, 3H; 21- $\text{CH}_3$ ), 0.87 (s, 3H; 19- $\text{CH}_3$ ), 0.61 ppm (s, 3H; 18- $\text{CH}_3$ ); <sup>13</sup>C NMR (300 MHz,  $[\text{D}_6]\text{DMSO}$ ):  $\delta$  = 172.5, 140.0, 137.9, 121.7, 85.7, 71.9, 71.1, 55.00, 54.96, 41.8, 41.3, 39.5, 39.3, 35.0, 34.6, 33.5, 30.4, 29.5, 27.3, 26.2, 25.4, 23.3, 22.4, 19.7, 17.5, 12.0 ppm; HRMS (ESI):  $m/z$  calcd for  $[\text{C}_{30}\text{H}_{44}\text{INO}_2+\text{H}]^+$ : 578.2495; found: 578.2489.

**OPE1:**  $[\text{Pd}(\text{Ph}_3\text{P})_4]$  (46.0 mg, 0.04 mmol) and CuI (7.6 mg, 0.04 mmol) were added to a stirred solution of **4** (632.2 mg, 1 mmol) and 1,4-diethynylbenzene (64.3 mg, 0.51 mmol) in DMF (10 mL) under nitrogen. The reaction mixture was stirred under nitrogen at 40°C for 20 h, then filtered. The filtrate was evaporated under vacuum and further purified by chromatography on neutral  $\text{Al}_2\text{O}_3$  ( $\text{CHCl}_3/\text{CH}_3\text{OH}$  15:1). The crude product was dissolved in a small amount of THF and added dropwise into acetone. OPE1 was obtained as a light yellow solid by filtration and was dried under vacuum for 24 h (337.6 mg, 62%). <sup>1</sup>H NMR (300 MHz,  $[\text{D}_6]\text{DMSO}$ ):  $\delta$  = 10.08 (s, 2H; NH), 7.65 (d,  $J$  = 7.2 Hz, 4H; Ar-H), 7.55 (s, 4H; Ar-H), 7.49 (d,  $J$  = 7.2 Hz, 4H; Ar-H), 4.32 (d,  $J$  = 4.2 Hz, 2H; 12-OH), 4.12 (d,  $J$  = 3.9 Hz, 2H; 7-OH), 4.05 (d,  $J$  = 3.8 Hz, 2H; 3-OH), 3.80 (s, 2H; 12-CH), 3.62 (s, 2H; 7-CH), 3.19–3.26 (m, 2H; 3-CH), 1.00–2.38 (m, 48H; alkyl-H), 0.98 (d,  $J$  = 5.6 Hz, 6H; 18- $\text{CH}_3$ ), 0.81 (s, 6H; 19- $\text{CH}_3$ ), 0.60 ppm (s, 6H; 21- $\text{CH}_3$ ); <sup>13</sup>C NMR (300 MHz,  $[\text{D}_6]\text{DMSO}$ ):  $\delta$  = 172.6, 140.6, 132.7, 132.0, 120.0, 119.0, 118.7, 92.2, 88.8, 71.5, 71.0, 66.8, 46.6, 46.3, 41.9, 36.3, 35.8, 35.7, 35.5, 34.1, 32.1, 31.9, 29.1, 27.8, 26.8, 23.4, 23.2, 17.0, 12.9 ppm; IR (KBr):  $\tilde{\nu}$  = 3428, 2923, 2862, 2215, 1669, 1593, 1520, 1046  $\text{cm}^{-1}$ ; MS (ESI):  $m/z$ : 1112  $[\text{M}+\text{Na}]^+$ ; elemental analysis calcd (%) for  $\text{C}_{70}\text{H}_{92}\text{N}_2\text{O}_8$ : C 77.17, H 8.51, N 2.57; found: C 76.93, H 8.90, N 2.41.

**OPE2:** OPE2 was synthesized as described for OPE1 by using **5** instead of **4**. Yield: 68%; <sup>1</sup>H NMR (300 MHz,  $[\text{D}_6]\text{DMSO}$ ):  $\delta$  = 10.08 (s, 2H; NH), 7.65 (d,  $J$  = 7.2 Hz, 4H; Ar-H), 7.55 (s, 4H; Ar), 7.49 (d,  $J$  = 7.2 Hz, 4H; Ar-H), 4.46 (d,  $J$  = 4.2 Hz, 2H; 12-OH), 4.20 (d,  $J$  = 3.9 Hz, 2H; 3-OH), 3.80 (s, 2H; 12-CH), 3.33–3.48 (m, 2H; 3-CH, overlap with the water signal in  $[\text{D}_6]\text{DMSO}$ ), 0.85–2.37 (m, 52H; alkyl-H), 0.91 (d,  $J$  = 6.0 Hz, 6H; 21- $\text{CH}_3$ ), 0.85 (s, 6H; 19- $\text{CH}_3$ ), 0.61 ppm (s, 6H; 18- $\text{CH}_3$ ); <sup>13</sup>C NMR (300 MHz,  $[\text{D}_6]\text{DMSO}$ ):  $\delta$  = 172.6, 140.6, 132.7, 132.0, 123.0, 119.4, 116.5, 92.2, 88.7, 71.6, 70.5, 48.0, 46.7, 46.5, 36.8, 36.2, 35.6, 34.4, 34.1, 33.5, 31.9, 30.8, 29.2, 27.7, 27.5, 26.7, 24.1, 23.6, 17.7, 13.0 ppm; IR (KBr):  $\tilde{\nu}$  = 3412, 2934, 2862, 2214, 1670, 1591, 1520, 1041, 838  $\text{cm}^{-1}$ ; MS (ESI):  $m/z$ : 1080  $[\text{M}+\text{Na}]^+$ ; elemental analysis calcd (%) for  $\text{C}_{70}\text{H}_{92}\text{N}_2\text{O}_6$ : C 79.50, H 8.77, N 2.65; found: C 79.00, H 8.52, N 2.94.

**OPE3:** OPE3 was synthesized as described for OPE1 by using **6** instead of **4**. Yield: 55%; <sup>1</sup>H NMR (300 MHz,  $[\text{D}_6]\text{DMSO}$ ):  $\delta$  = 10.07 (s, 2H; NH), 7.65 (d,  $J$  = 7.2 Hz, 4H; Ar-H), 7.54 (s, 4H; Ar-H), 7.48 (d,  $J$  = 7.2 Hz, 4H; Ar-H), 4.41 (s, 2H; 3-OH), 3.20–3.50 (m, 2H; 3-CH), 1.02–1.93 (m, 60H; alkyl-H), 0.94 (d,  $J$  = 5.6 Hz, 6H; 18- $\text{CH}_3$ ), 0.87 (s, 6H; 19- $\text{CH}_3$ ), 0.61 ppm (s, 6H; 21- $\text{CH}_3$ ); <sup>13</sup>C NMR (300 MHz,  $[\text{D}_6]\text{DMSO}$ ):  $\delta$  = 172.4, 141.1, 136.0, 132.7, 119.9, 118.0, 92.2, 71.0, 57.1, 56.2, 43.0, 42.3, 41.3, 40.5, 36.3, 35.9, 34.5, 32.8, 31.1, 29.1, 27.7, 26.5, 23.7, 23.1, 21.4, 17.0, 11.9 ppm; IR (KBr):  $\tilde{\nu}$  = 3481, 3426, 2930, 2850, 2214, 1672, 1585, 1527  $\text{cm}^{-1}$ ; MS (ESI):  $m/z$ : 1048  $[\text{M}+\text{Na}]^+$ ; elemental analysis calcd (%) for  $\text{C}_{70}\text{H}_{92}\text{N}_2\text{O}_4$ : C 81.99, H 9.04, N 2.73; found: C 81.56, H 9.49, N 2.52.

## Acknowledgements

We gratefully acknowledge the financial support from the National Science Foundation of China (20533050, 20772071, and 50673048), 973 Program (2006CB806200) and the transregional project (TRR6). We would also like to thank Prof. Chun Li for help during the circular dichroism experiment.

- [1] a) M. Grell, D. D. C. Bradley, *Adv. Mater.* **1999**, *11*, 895–905; b) J. A. A. W. Elemans, R. van Hameren, R. J. M. Nolte, A. E. Rowan, *Adv. Mater.* **2006**, *18*, 1251–1266; c) U. H. F. Bunz, *Chem. Rev.* **2000**, *100*, 1605–1644.
- [2] a) M. J. Plater, J. P. Sinclair, S. Aiken, T. Gelbrich, M. B. Hursthouse, *Tetrahedron* **2004**, *60*, 6385–6394; b) B. Francesco, C. Donato, D. B. Lorenzo, M. F. Gianluca, H. O. Omar, N. Francesco, P. Gennaro, *Macromolecules* **2006**, *39*, 5206–5212.
- [3] Y. Li, J. R. Dias, *Chem. Rev.* **1997**, *97*, 283–304.
- [4] a) J. Wu, T. Yi, T. Shu, M. Yu, Z. Zhou, M. Xu, Y. Zhou, H. Zhang, J. Han, F. Li, C. Huang, *Angew. Chem.* **2008**, *120*, 1079–1083; *Angew. Chem. Int. Ed.* **2008**, *47*, 1063–1067; b) X. Wang, Y. Lu, Y. Duan, L. Meng, C. Li, *Adv. Mater.* **2008**, *20*, 462–465.
- [5] a) S. Kawano, N. Fujita, S. Shinkai, *Chem. Eur. J.* **2005**, *11*, 4735–4742; b) P. Xue, R. Lu, D. Li, M. Jin, C. Bao, Y. Zhao, Z. Wang, *Chem. Mater.* **2004**, *16*, 3702–3707.
- [6] M. S. Neralagatta, U. Maitra, *Chem. Soc. Rev.* **2005**, *34*, 821–836.
- [7] Y. Li, G. Li, X. Wang, C. Lin, Y. Zhang, Y. Ju, *Chem. Eur. J.* **2008**, *14*, 10331–10339.
- [8] M. Shibakami, M. Tamura, A. Sekiya, *J. Am. Chem. Soc.* **1995**, *117*, 4499–4505.
- [9] a) F. Brustolin, F. Goldoni, E. W. Meijer, N. A. J. M. Sommerdijk, *Macromolecules* **2002**, *35*, 1054–1059; b) R. Iwaura, F. J. M. Hoeben, M. Masuda, A. P. H. J. Schenning, E. W. Meijer, T. Shimizu, *J. Am. Chem. Soc.* **2006**, *128*, 13298–13304.
- [10] S. Verma, T. Hauck, M. E. El-Khouly, P. A. Padmawar, T. Canteenwala, K. Pritzker, O. Ito, L. Y. Chiang, *Langmuir* **2005**, *21*, 3267–3272.
- [11] J. H. Fuhrhop, H. H. David, J. Mathieu, U. Liman, H. J. Winter, E. Boekema, *J. Am. Chem. Soc.* **1986**, *108*, 1785–1791.
- [12] DLS measurements may slightly overestimate the size of the particles due to agglomeration in aqueous solution.

- [13] A. Ajayaghosh, C. Vijayakumar, R. Varghese, S. J. George, *Angew. Chem.* **2006**, *118*, 470–474; *Angew. Chem. Int. Ed.* **2006**, *45*, 456–460.
- [14] L. Li, H. Jiang, B. W. Messmore, S. R. Bull, S. I. Stupp, *Angew. Chem.* **2007**, *119*, 5977–5980; *Angew. Chem. Int. Ed.* **2007**, *46*, 5873–5876.
- [15] a) Y. Zhao, *Curr. Top. Mol. Simul. Curr. Opin. Colloid. Interface Sci.* **2007**, *12*, 92–97; b) V. H. S. Tellini, A. Jover, F. Meijide, J. V. Tato, L. Galantini, N. V. Pavel, *Adv. Mater.* **2007**, *19*, 1752–1756.
- [16] S. H. Seo, J. Y. Chang, G. N. Tew, *Angew. Chem.* **2006**, *118*, 7688–7692; *Angew. Chem. Int. Ed.* **2006**, *45*, 7526–7530.
- [17] M. Alvarez Alcalde, A. Jover, F. Meijide, L. Galantini, N. V. Pavel, A. Antelo, J. Tato, *Langmuir* **2008**, *24*, 6060–6066.
- [18] Y. Wang, B. Erdogan, J. N. Wilson, U. H. F. Bunz, *Chem. Commun.* **2003**, 1624–1625.
- [19] T. Kaneko, A. Ichikawa, J. P. Gong, Y. Osada, *Macromol. Rapid Commun.* **2003**, *24*, 789–792.
- [20] a) Nonappaa, U. Maitra, *Org. Biomol. Chem.* **2008**, *6*, 657–669; b) L. B. Partay, M. Sega, P. Jedlovszky, *Langmuir* **2008**, *24*, 10729–10736.
- [21] a) A. Rich, D. M. Blow, *Nature* **1958**, *182*, 423–426; b) N. Ramathan, A. L. Currie, J. R. Colvin, *Nature* **1961**, *190*, 779–781.
- [22] M. J. Plater, J. P. Sinclair, S. Aiken, T. Gelbrich, M. B. Hursthouse, *Tetrahedron* **2004**, *60*, 6385–6394.

Received: February 22, 2009  
Published online: May 26, 2009